European Journal of Technique

journal homepage: https://dergipark.org.tr/en/pub/ejt

Vol.14, No.1, 2024

Research Article

Optimization of Optimal Power Flow considering Location of FACTS Devices using Partial Reinforcement Optimizer

Burçin Özkaya[1*]

[1*] Bandirma Onyedi Eylul University, Electrical Engineering Department, 10200, Bandırma, Balıkesir, Turkey. (e-mail: bozkaya@bandirma.edu.tr).

ARTICLE INFO

Received: May., 06. 2024
Revised: June., 11. 2024
Accepted: June., 13. 2024

Keywords:
Optimization
Partial reinforcement optimizer
Optimal power flow
FACTS devices

Corresponding author: *Burçin Özkaya*

ISSN: *2536-5010* | e-ISSN: *2536-5134*

DOI:
https://doi.org/10.36222/ejt.1479409

ABSTRACT

Optimal power flow (OPF) is the most commonly addressed modern power system planning and operating optimization problem. It becomes a very difficult and high complexity optimization problem with the inclusion of the optimal location and sizing of flexible AC transmission system (FACTS) devices. Therefore, to obtain the optimal solution for the OPF problem, it is necessary to use the most suitable meta-heuristic search (MHS) algorithm. In this study, an up-to-date and strong MHS algorithm known as the partial reinforcement optimizer (PRO) was used to solve the OPF problem considering optimal location and sizing of the multi-type FACTS devices. The objectives considered in the study were minimization of total cost, minimization of total cost with valve-point loading effect, and minimization of the real power loss. In the simulation studies, four case studies were considered and solved by PRO algorithm and its three rivals including dingo optimization algorithm, evolutionary mating algorithm, and snow geese algorithm. According to the results of the case studies, compared to its closest competitor, the evolutionary mating algorithm algorithm, its objective function values for Case-1, Case-2, Case-3, and Case-4 were lower by 0.0059%, 0.2814%, 0.0062%, and 0.0003%, respectively. The performance of PRO algorithm was evaluated using Friedman and Wilcoxon tests against its rivals. The Friedman test results show that PRO algorithm achieved the best rank first with 1.2333 score value among them. In summary, PRO algorithm achieved superior performance in solving these case studies.

1. INTRODUCTION

One of the most significant operating and planning issues in modern power systems is optimal power flow (OPF). Because of the nonlinear power flow equations, generator cost curves, and operational limitations, it is usually defined as a non-convex and nonlinear optimization problem. Its aim is to minimize the objective function while meeting a variety of operational limitations to specify the optimal operating conditions for a power system, usually an electrical grid, by adjusting control variables [1-3].

In power system operations, the absence of reactive power causes problems such as voltage fluctuations, reduction, collapse, and instability. Moreover, the generators and capacitor banks generate reactive power at a slow pace, making it challenging to adapt to sudden load changes. Therefore, flexible alternating current transmission system (FACTS) devices have an important role, such as controlling the power flow, increasing the power loss, and solving operational problems including congestion, voltage fluctuations, and line losses, and as to improve power system stability, transmission efficiency, and grid reliability [4]. In fact, FACTS devices can control many parameters of transmission lines; the most important of these are the shunt impedance, series impedance, and phase angles. FACTS devices are very helpful for a power system; however, the OPF problem with FACTS devices is challenging because of the complexity, nonlinearities, non-convexity, and modeling accuracy required for an accurate solution [3-5]. Therefore, meta-heuristic search (MHS) algorithms have been used by researchers in the literature to solve the OPF problem including FACTS devices. Some of MHS algorithms used for the solution of the OPF including FACTS devices were the lightning search algorithm [1], the krill herd algorithm [3], the enhanced bacterial foraging algorithm [5], the symbiotic organisms search algorithm [6], the new partitioned ant lion optimizer [7], the modified Runge Kutta optimizer [8], the lightning attachment procedure optimization [9], etc.

In the above mentioned research, FACTS devices were placed on fixed branches in the power system. However, the placement and sizing of the FACTS devices directly affect the power flow, voltage profiles, system stability, and overall grid performance [2, 10]. The optimal allocation of FACTS

devices can optimize the power flow, minimize the power losses, and improve the voltage stability. To sum up, the placement of the FACTS devices for the OPF problem is crucial for the efficient, reliable and cost-effective operation of power systems [10, 11]. The optimal placement and ratings of the FACTS devices for the OPF problem can be considered highly constrained, multimodal, and complex optimization problems.

In the literature, the optimal placement of FACTS devices in optimal power flow has been solved using MHS algorithms. Sulaiman and Mustaffa presented a comprehensive study using seven MHS algorithms in solving the OPF problem considering the optimal placement and rating of the TCSC and SVC devices on IEEE 14-bus test system [2]. Biswas et al. performed optimal power flow incorporating wind energy sources and multi-type FACTS devices using the success history-based adaptive differential evolution [10]. Inkollu and Kota proposed a hybrid algorithm to improve the voltage stability of the system and optimize the placement of the FACTS devices [12]. Sakr et al. proposed an adaptive differential evolution algorithm to optimize the location of the TCSC in the network [13]. Ziaee and Choobineh modeled the location of the TCSC problem as a mixed integer nonlinear program and Benders' decomposition method was used to solve the problem [14]. Raj and Bhattacharyya presented a comparative study using five different MHS algorithms for solving the reactive power planning with FACTS devices. Moreover, the optimal location of the TCSC and static VAR compensator (SVC) was determined [15]. In another study, Agrawal et al. presented a comparative study for the optimal location and sizing of the TCSC using evolutionary optimization techniques. The performance of the algorithms was tested on IEEE 14-bus, 30-bus, and 75-bus systems [16]. Khan et al. proposed a modified lightning attachment procedure optimizer for solving the optimal reactive power dispatch including TCSC and SVC devices. In this study, the optimal placement of them were also considered [17]. Nusair et al. performed a comprehensive study about the solution of the OPF problems including multi-type FACTS devices and wind renewable energy sources using four MHS algorithms [18]. Mohamed et al. proposed a hybrid algorithm including a gradient-based optimizer and a moth flame optimization algorithm to solve the OPF considering optimal allocation and rating of multi-type FACTS devices and wind power [19]. Hassan et al. introduced an enhanced hunter-prey optimization algorithm to solve the OPF problem including wind energy sources and FACTS devices such as SVC, TCSC, and thyristor-controlled phase shifter (TCPS). Here, the optimal location and sizing of the FACTS devices were also considered in the OPF problem [20]. Awad et al. proposed the der-based walrus optimization algorithm for solving the OPF problems on the IEEE 30-bus test system. The optimal location of multi-type of FACTS devices were also considered [21]. Mohamed et al. introduced chaotic african vultures optimization algorithm for solving the OPF problem incorporating wind power and multi-type FACTS devices. The objectives were the minimization of generation cost and minimization of active power loss. Moreover, the optimal location and rating of the FACTS devices were optimized [22]. Mahapatra et al. presented a hybrid cuckoo search algorithm and ant-lion optimizer for determining the optimal placement and sizing of the TCSC. In the study, the placement and sizing of the TCSC were determined by using CS and ALO algorithms, respectively [23].

In this study, the OPF problem including multi-type FACTS devices was solved by using partial reinforcement optimizer (PRO). The PRO algorithm was introduced to the literature by Taheri et al. in 2024 [24]. In the OPF problem, three objective functions were considered: (i) minimization of total cost, (ii) minimization of total cost with the valve-point loading effect, (iii) minimization of the real power loss. On the other hand, the allocation and rating of the TCSC and TCPS devices were determined to minimize the relevant objective function. Accordingly, four different case studies were carried out on the IEEE 30-bus test system using the objective functions and FACTS devices. The performance of the PRO algorithm was compared with the dingo optimization algorithm (DOA) [25], the evolutionary mating algorithm (EMA) [26], and the snow geese algorithm (SGA) [27]. Accordingly, the contributions of this study can be summarized as follows:

- The PRO algorithm was applied to solve the OPF problem considering location and sizing of the FACTS devices.
- Four different case studies were considered using the three objective functions and two FACTS devices.
- The performance of the PRO algorithm was compared with the up-to-date three MHS algorithms.
- A comprehensive analysis was performed using the convergence analysis and statistical analysis methods to prove the performance of the PRO algorithm in solving the OPF problem against its rivals.

The remaining sections of the paper are organized as follows: Section 2 presents the formulation of the problem, where the modeling of the TCSC and TCPS devices, the objective functions and the constraints considered in the OPF problem are defined. In section 3, the partial reinforcement optimizer is explained. Section 4 presents the simulation studies and results. Moreover, the results of the case studies, the convergence and the statistical analysis results were given. Section 5 presents the conclusion of the study.

2. FORMULATION OF THE PROBLEM

The primary goal of the OPF problem is to minimize the objective function to determine the optimal control variables, taking into account the equality and inequality constraints. It is typically expressed as in Eq. (1).

$$\begin{aligned} &Minimize \quad OF(\boldsymbol{v},\boldsymbol{u}) \\ &subject\ to \begin{cases} H(\boldsymbol{v},\boldsymbol{u}) = 0 \\ G(\boldsymbol{v},\boldsymbol{u}) \le 0 \end{cases} \end{aligned} \tag{1}$$

Here, *OF*, *G*, and *H* represent the objective function, the inequality and equality constraints, respectively. Also, $\boldsymbol{u}$ and $\boldsymbol{v}$ denote the control and state variables vector, respectively [1, 6].

In this study, the placement of TCSC and TCPS devices presented in section 2 is considered. The placement and sizing of these devices are optimized to minimize the related objective function. Accordingly, the state and control variables of this problem are expressed as follows:

$$\boldsymbol{u} = \begin{bmatrix} P_{THG_2} \dots P_{THG_{NTHG}}, V_{G_1} \dots V_{G_{NTHG}}, T_1 \dots T_{N_T}, \\ TCSC_1 \dots TCSC_m, \tau_{TCSC_1} \dots \tau_{TCSC_m}, \\ TCPS_1 \dots TCPS_p, \phi_{TCPS_1} \dots \phi_{TCPS_p} \end{bmatrix} \tag{2}$$

$$\boldsymbol{v}=\left[P_{THG_1},V_{L_1}\ldots V_{L_{N_{PQ}}},Q_{THG_1}\ldots Q_{THG_{N_{THG}}},S_{L_1}\ldots S_{L_{N_{TL}}}\right] \quad (3)$$

where P_{THG}, Q_{THG}, and V_G active power, reactive power, and the voltages of the thermal generating units. T is the tap changing transformer settings, V_L is the voltage of the load buses, S_L is the transmission line loading. N_{THG}, N_T, N_{TL}, m, and p are the number of the transformers, the number of thermal generating units, the number of transmission lines, the number of TCSC devices, and the number of TCPS devices, respectively.

2.1. Modeling of FACTS devices

In this study, the thyristor-controlled phase shifter (TCPS) and thyristor-controlled series capacitor (TCSC) devices were considered, which are used to increase the power flow and loading ability of the line. This section includes two sub-sections, where the modeling of the TCSC and TCPS devices is presented.

2.1.1. Modeling of TCSC device

TCSC is used in power systems to enhance the system performance and control the power flow. The circuit model of the TCSC between the i^{th} and k^{th} buses in a power grid is given in Fig. 1. The equivalent reactance (X_{eq}) of the transmission line is given as follows [6]:

$$X_{eq}=X_{ik}-X_{TCSC}=X_{ik}(1-\tau) \quad (4)$$

where X_{ik} and X_{TCSC} are the inductive reactance of the line and TCSC devices, respectively. τ is called the series compensation degree with X_{ik}.

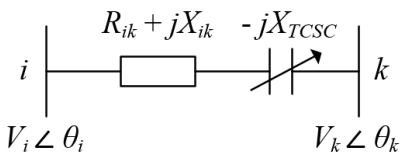

Figure 1. Circuit model of TCSC

The power flow equations between i^{th} and k^{th} buses including TCSC can be written as follows [6]:

$$P_{ik}=V_i^2G_{ik}-V_iV_kG_{ik}\cos(\theta_{ik})-V_iV_kB_{ik}\sin(\theta_{ik}) \quad (5)$$

$$Q_{ik}=-V_i^2B_{ik}-V_iV_kG_{ik}\sin(\theta_{ik})+V_iV_kB_{ik}\cos(\theta_{ik}) \quad (6)$$

$$P_{ki}=V_k^2G_{ik}-V_iV_kG_{ik}\cos(\theta_{ik})+V_iV_kB_{ik}\sin(\theta_{ik}) \quad (7)$$

$$Q_{ki}=-V_k^2B_{ik}+V_iV_kG_{ik}\sin(\theta_{ik})+V_iV_kB_{ik}\cos(\theta_{ik}) \quad (8)$$

where P_{ik} and Q_{ik} are the active and reactive power flows from i^{th} to k^{th} bus, θ_k and θ_i are the angles of the k^{th} and i^{th} buses, V_k and V_i are the voltages of the k^{th} and i^{th} buses, respectively.

The conductance (G_{ik}) and the susceptance (B_{ik}) of the transmission line are computed as follows [6]:

$$G_{ik}=\frac{X_{ik}}{X_{ik}^2+X_{new}^2},\ B_{ik}=-\frac{X_{new}}{X_{ik}^2+X_{new}^2} \quad (9)$$

2.1.2. Modeling of TCPS device

TCPS can be modelled using a phase-shifting transformer with control parameter (Φ) in the power system [6]. The circuit model of the TCPS between i^{th} and k^{th} bus in a power grid is shown in Fig. 2.

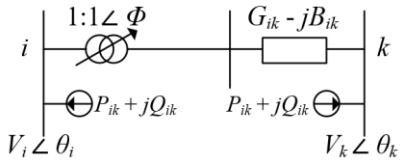

Figure 2. Circuit model of TCPS

The power flow equations between i^{th} and k^{th} bus including TCPS can be expressed as follows [6]:

$$P_{ik}=\frac{V_i^2G_{ik}}{\cos^2\phi}-\frac{V_iV_k}{\cos\phi}\left[B_{ik}\sin(\theta_{ik}+\phi)+G_{ik}\cos(\theta_{ik}+\phi)\right] \quad (10)$$

$$Q_{ik}=-\frac{V_i^2B_{ik}}{\cos^2\phi}-\frac{V_iV_k}{\cos\phi}\left[-B_{ik}\cos(\theta_{ik}+\phi)+G_{ik}\sin(\theta_{ik}+\phi)\right] \quad (11)$$

$$P_{ki}=V_k^2G_{ik}-\frac{V_iV_k}{\cos\phi}\left[-B_{ik}\sin(\theta_{ik}+\phi)+G_{ik}\cos(\theta_{ik}+\phi)\right] \quad (12)$$

$$Q_{ki}=-V_k^2B_{ik}+\frac{V_iV_k}{\cos\phi}\left[B_{ik}\cos(\theta_{ik}+\phi)+G_{ik}\sin(\theta_{ik}+\phi)\right] \quad (13)$$

The injected reactive and active power of TCPS at i^{th} and k^{th} bus is written as [6]:

$$P_{is}=-V_i^2G_{ik}\tan^2\phi-V_iV_k\tan\phi\left[-B_{ik}\cos\theta_{ik})+G_{ik}\sin(\theta_{ik})\right] \quad (14)$$

$$Q_{is}=V_i^2B_{ik}\tan^2\phi+V_iV_k\tan\phi\left[B_{ik}\sin(\theta_{ik})+G_{ik}\cos(\theta_{ik})\right] \quad (15)$$

$$P_{ks}=-V_iV_k\tan\phi\left[B_{ik}\cos(\theta_{ik})+G_{ik}\sin(\theta_{ik})\right] \quad (16)$$

$$Q_{ks}=-V_iV_k\tan\phi\left[-B_{ik}\sin(\theta_{ik})+G_{ik}\cos(\theta_{ik})\right] \quad (17)$$

2.2. Objective functions

In this study, three objective functions are considered.

(i) *Minimization of the total cost*: The cost of the thermal generating units is expressed as in Eq. (18), where $\alpha_j,\beta_j,\delta_j$ are the cost coefficients of the j^{th} thermal generating unit. P_{THG} is the active power of the j^{th} thermal generating unit and N_{THG} is the number of thermal generating units [1].

$$OF_1=\sum_{j=1}^{N_{THG}}\alpha_j+\beta_jP_{THG_j}+\delta_jP_{THG_j}^2 \quad (18)$$

(ii) *Minimization of the total cost including valve-point loading effect*: The total cost including VPLE of the thermal generating units can be expressed as in Eq. (19). Here, x_j and

y_j are the coefficients of valve-point loading of the j^{th} thermal generating unit [1].

$$OF_2 = \sum_{j=1}^{N_{THG}} \alpha_j + \beta_j P_{THG_j} + \delta_j P_{THG_j}^2 + \left| x_j \times \sin\left(y_j \times \left(P_{THG_j}^{\min} - P_{THG_j} \right) \right) \right| \quad (19)$$

(iii) *Minimization of active power loss*: It can be mathematically expressed as in Eq. (20), where *i* and *k* are the bus in a power grid [1].

$$OF_3 = \sum_{l=1}^{N_{TL}} G_{m(ik)} \left(V_i^2 + V_k^2 - 2V_i V_k \cos(\theta_{ik}) \right) \quad (20)$$

2.3. Constraints

Equality constraints: The equality constraints defined as follows [6]:

$$P_{G_i} - P_{D_i} + P_{is} = V_i \sum_{k=1}^{N_B} V_k Y_{ik} \cos(\psi_{ik} + \theta_{ik}), \ \forall i \in N_B \quad (21)$$

$$Q_{G_i} - Q_{D_i} + Q_{is} = V_i \sum_{k=1}^{N_B} V_k Y_{ik} \sin(\psi_{ik} + \theta_{ik}), \ \forall i \in N_B \quad (22)$$

where P_{D_i} and Q_{D_i} represent the active and reactive power load demand, respectively. Q_{G_i} and P_{G_i} are the reactive and active power of the i^{th} generating unit, respectively. N_B denotes the number of buses. P_{is} and Q_{is} are the injected active and reactive power by the TCPS of the m^{th} bus, respectively. ψ_{ik} is the angle value of the ik^{th} element of the bus admittance matrix and Y_{ik} is the magnitude of it.

Inequality constraints [6]:

- Generator constraints:

$$\begin{aligned} &P_{THG_i,min} \le P_{THG_i} \le P_{THG_i,max}, \ \forall i \in N_{THG} \\ &Q_{THG_i,min} \le Q_{THG_i} \le Q_{THG_i,max}, \ \forall i \in N_{THG} \\ &V_{G_i,min} \le V_{G_i} \le V_{G_i,max}, \ \forall i \in N_G \end{aligned} \quad (23)$$

- Security constraints:

$$S_{L_i} \le S_{L_i,max}, \ \forall i \in N_{TL} \quad (24)$$

$$V_{L_i,min} \le V_{L_i} \le V_{L_i,max}, \ \forall i \in N_{PQ} \quad (25)$$

- Transformer constraints:

$$T_{j,min} \le T_j \le T_{j,max}, \ \forall j \in N_T \quad (26)$$

- TCSC and TCPS constraints:

$$\tau_{TCSC_r}^{\min} \le \tau_{TCSC_r} \le \tau_{TCSC_r}^{\max}, \ \forall r \in m \quad (27)$$

$$\phi_{TCPS_z}^{\min} \le \phi_{TCPS_z} \le \phi_{TCPS_z}^{maz}, \ \forall z \in p \quad (28)$$

2.4. Constraint handling method

The widely used constraint avoidance technique for solving OPF problems with MHS algorithms is the penalty function method. In this method, the constraint violation values are added to the objective function value in an attempt to modify each infeasible individual's fitness status [28]. Accordingly, the fitness function obtained by adding the constraint violation values to the objective functions discussed in this study using the penalty function method can be expressed with Equation (29). Here, $Fitness_i$ and $F_{penalty,i}$ represent the fitness function and the penalty function of the i^{th} objective function. γ_1, γ_2, γ_3, γ_4, γ_5, and γ_6 are the penalty coefficients.

$$Fitness_i = OF_i + F_{penalty,i} = OF_i + \begin{bmatrix} \gamma_1 \sum_{j=1}^{N_B} \left(P_{G_i} - P_{D_i} + P_{is} \right) + \gamma_2 \sum_{j=1}^{N_B} \left(Q_{G_i} - Q_{D_i} + Q_{is} \right) + \\ \gamma_3 \left(P_{THG_1} - P_{THG_1}^{lim} \right) + \gamma_4 \left(Q_{THG_1} - Q_{THG_1}^{lim} \right) + \\ \gamma_5 \sum_{i=1}^{N_{PQ}} \left(V_{L_i} - V_{L_i}^{lim} \right) + \gamma_6 \sum_{i=1}^{N_{TL}} \left(S_{L_i} - S_{L_i}^{lim} \right) \end{bmatrix} \quad (29)$$

3. PARTIAL REINFORCEMENT OPTIMIZER

Partial Reinforcement Optimizer (PRO) was presented to the literature in 2024 by Taheri et al. [24]. Its inspiration is the Partial Reinforcement Extinction (PRE) theory presented by Ferster and Skinner in 1957 [29]. In the PRO algorithm, there are some basic concepts that need to be defined before examining the structure of it: learner, behavior, population, and response. A learner refers to an individual or animal whose behaviors require training through the PRE theory, and a solution represents the learner. The behavior of the learners is viewed as a solution involving decision variables. The group of learners forms the population. A response refers to the prospective improvement in the objective function.

The PRO algorithm includes three important stages: schedule, stimulation, and reinforcement, which are explained as follows [24]:

Schedule: The idea behind a schedule is to model behaviors for a data structure at different intervals and determine when and how they should be reinforced. Each learner has their own schedule. The scale used in this schedule indicates the priority or score of the behavior of the learner; higher scores mean a better chance of selection in the next round. Furthermore, a stochastic analysis is represented dynamically using the variable-interval scheduling method using Eqns. (30)-(32).

During the search process, the schedule's priorities are sorted from highest to lowest, and a subset of behaviors with the highest priorities for each learner is chosen in each iteration. This subset, which serves as the candidate behaviors utilizing Eq. (31) is made up of the first λ items depending on priority [24].

$$\tau = \frac{FEs}{maxFEs} \quad (30)$$

$$SR = e^{-(1-\tau)} \quad (31)$$

$$\mu \subseteq \{1,2,...,N\} \mid \forall j \in \mu, schedule^j \ge schedule^{*,\lambda}, \quad \lambda = \left\{ \|\mu\| \mid \|\mu\| = \left[u(1, N \times SR) \right] \right\} \quad (32)$$

Here, *FEs* and *maxFEs* are the number of fitness function evaluations and the maximum number of FEs, respectively. τ, μ, λ, *SR*, and *N* are the time factor, a subset of behaviors chosen in accordance with scheduling, the selected subset's size, the selection rate, and the number of behaviors, respectively. $schedule^{*}$ and $schedule^{*,\lambda}$ represent the prioritized schedule and the λ^{th} item in the $schedule^{*}$.

Stimulation: Applying operations that change the decision variables of a proposed solution represents an attempt to elicit a response from the behaviors of the learners. In the PRO algorithm, these operations are used to produce the new solutions performed by Eqns. (33)-(35). Here, the decision factors chosen for the student based on the scheduler are represented by the symbols SF_i and $\overline{\beta}$, which stand for the stimulation factor and the mean value of the normalized score, respectively [24].

$$SF_i = \tau + u\left(0,\overline{\beta}\right), \text{ where } \overline{\beta} = \sum_{j\in\mu}\left(\frac{schedule_{i,j}}{\max\left(schedule_i\right)}\right) \tag{33}$$

$$S_i^{\mu} = \begin{cases}\left(x_{best}^{\mu} - x_i^{\mu}\right), & if\ \ rand < 0.5\\ \left(x_i^{\mu} - x_j^{\mu}\right), & otherwise\end{cases} \tag{34}$$

$$x_{i,new}^{\mu} = x_i^{\mu} + SF_i \times S_i^{\mu} \tag{35}$$

Reinforcement: The PRO algorithm uses both positive and negative reinforcement. A certain behavior's score is raised by the application of positive reinforcement. Following improvement during the stimulation phase, the learner's objective function, as stated in Eq. (36) is employed as a response. Here, $schedule_j^{\mu}$ denotes the priority of the chosen behaviors for the j^{th} learner and *RR* is the reinforcement rate [24].

$$schedule_j^{\mu} = schedule_j^{\mu} + \left(schedule_j^{\mu} \times RR\right) \tag{36}$$

Conversely, negative reinforcement is applied in the absence of a response, which lowers the behavior's score and objective function. In the following iteration, only the behaviors with higher scores are chosen to receive reinforcement and stimulation.

$$schedule_j^{\mu} = schedule_j^{\mu} - \left(schedule_j^{\mu} \times RR\right) \tag{37}$$

Rescheduling: This process entails introducing a new timetable for a learner, with the learner consistently receiving negative reinforcement for all behaviors during training. The PRO uses the schedule's standard deviation to assess when rescheduling the learner is necessary. This procedure is implemented using Eqns. (38) and (39) [24].

$$schedule_j = \begin{cases}u(0,1), & if\ \ std\left(schedule_j\right) = 0\\ \text{Do nothing}, & else\end{cases} \tag{38}$$

$$x_j = \begin{cases}u\left(l_b,u_b\right), & if\ \ std\left(schedule_j\right) = 0\\ \text{Do nothing}, & else\end{cases} \tag{39}$$

Here, std is the abbreviation of the standard deviation, l_b and u_b represent the lower and upper bound, respectively. $u(l_b, u_b)$ and $u(0,1)$ denote the randomly uniform distributed values between the (l_b, u_b) and (0,1), respectively.

The flowchart of the PRO algorithm is given in Algorithm-1.

Algorithm-1: The pseudocode of the PRO algorithm [24]

Inputs: Population size, *maxFEs*, *RR*

```
Initialize the population and schedules
Compute the responses of the learners in the population
while FEs<maxFEs
    for j = 1 : N      // for all learners
        Calculate the time parameter using Eq. (30)
        Calculate the SR using Eq. (31)
        Choose λ number of behaviors that have the highest priority
        in schedule j using Eq. (32)
        Update the β and SF based on Eqns. (33) and (34)
        Compute the x_{j,new}^{μ} using Eq. (35)
        Compute the response of j^th learner
              //Apply negative or positive reinforcement
                    based on the response//
        if F(x_{j,new}^{μ}) < F(x_j)
            x_j = x_{j,new}^{μ}
            Employ positive reinforcement using Eq. (36)
        else
            Employ negative reinforcement using Eq. (37)
        end if
        Update the best solution
        Perform the rescheduling process based on Eqns. (38) and
    (39)
        FEs = FEs+1
    end for
end while
```

4. SIMULATION STUDIES AND RESULTS

In this section, the performance of the PRO algorithm was investigated on the IEEE 30-bus test system with TCSC and TCPS devices. The IEEE 30-bus test system consists of six generators at buses 1, 2, 5, 8, 11, and 13 connected to each other with 41 transmission lines and four tap changing transformers. The detailed data of the IEEE 30-bus power network are obtained from [30]. The cost coefficients of the IEEE 30-bus test system are taken from [31].

The main purpose is to optimize the relevant objective function by placing FACTS devices in the optimal locations on the IEEE 30-bus test system. According to this, four different case studies were considered in this study and the summary of them is presented in Table 1. Table 1 provides information on which objective functions and which FACTS devices were used in the case studies.

TABLE I
CASE STUDIES USED IN THE STUDY

Case(s)	Objective Function			FACTS Devices	
	OF_1	OF_2	OF_3	TCSC	TCPS
Case-1	●			●	
Case-2			●	●	
Case-3	●			●	●
Case-4		●		●	●

When Table 1 was examined, two TCSC devices were added to the test system for Case-1 and Case-2, while two TCSC and two TCPS devices were added for Case-3 and Case-4. In these case studies, for each FACTS device, two control variables are assigned that represent the device's location and rating. The variables representing the location are discrete integers indicating the numbers of the branches and

buses, and are obtained by rounding to the nearest integer during the optimization process. Two criteria were taken as the basis for including the FACTS devices to the test system; (*i*) it is not possible to add two FACTS devices in the same location, (*ii*) TCSC and TCPS cannot be added to branches with tap changing transformers. In the case studies, the TCSC agreed to accept a 50% maximum compensation of the installed line reactance, and the lower and upper limits for the phase shifting angle for TCPS were -5° to +5°.

To compare the performance of the PRO algorithm for solving the OPF problem with TCSC and TCPS devices, three up-to-date MHS algorithms, which were the dingo optimization algorithm (DOA), the evolutionary mating algorithm (EMA), and the snow geese algorithm (SGA), were applied to solve all case studies. The parameters of the algorithms are presented in Table 2. The maximum number of fitness function evaluations (*maxFEs*) was set as 30000 for all case studies. Besides, all algorithms performed 30 runs for each case study.

TABLE II
PARAMETERS OF THE ALGORITHMS

Algorithm	Year	Parameter(s)
PRO [24]	2024	Number of population = 30, RR = 0.7
SGA [27]	2024	Number of population = 30,
EMA [26]	2022	Number of population = 30, Cr = 0.8
DOA [25]	2021	Number of population = 100, P=0.5, Q=0.7

4.1. Results of case studies

The PRO, DOA, EMA, and SGA algorithms were applied to solve the four case studies. All algorithms were performed 30 runs for all cases. Accordingly, the results obtained from them were assessed using the minimum (min), mean, maximum (max), and standard deviation (std). In Table 3, the min, max, mean, and std values of all algorithms for all case studies were tabulated.

TABLE III
THE RESULTS OF ALL ALGORITHMS FOR CASE STUDIES

Case(s)	Parameter	PRO	DOA	EMA	SGA
Case-1	Min	**800.7291**	801.1595	800.7766	801.0689
	Mean	**800.8452**	802.7512	802.8931	801.3670
	Max	800.9696	811.8790	818.2737	801.6416
	Std	0.0630	2.6984	5.1248	0.1595
Case-2	Min	**3.2112**	3.2629	3.2202	3.2486
	Mean	**3.2371**	3.5567	3.3629	3.3146
	Max	3.2886	4.6973	4.3397	3.5159
	Std	0.0226	0.3365	0.2809	0.0562
Case-3	Min	**800.6926**	801.3040	800.7419	801.0178
	Mean	**800.8189**	804.4709	801.7940	801.5760
	Max	800.9153	832.9893	803.9818	802.9945
	Std	0.0550	6.2821	1.1489	0.4639
Case-4	Min	**831.6959**	832.9082	831.6988	831.9242
	Mean	**831.9700**	840.2567	833.7043	833.7467
	Max	832.5879	873.2547	845.6788	837.5147
	Std	0.1972	10.5736	3.1634	1.4470

Case-1: *Minimization of the total cost with TCSC*

In this case, the objective was to minimize the total cost given in Eq. (18). The optimal variables obtained from the PRO algorithm for Case-1 are presented in Table 4. It can be seen from Table 4 that all control variables were within the specified lower and upper limit bounds. From Table 3, the total cost values of the PRO, DOA, EMA, and SGA were **800.7291 $/h**, **801.1595 $/h**, **800.7766 $/h**, and **801.0689 $/h**, respectively. That is, the total cost of the PRO was **0.0537%**, **0.0059%**, and **0.0424%** lower than the DOA, EMA, and SGA algorithms, respectively. On the other hand, according to the minimum cost values obtained by the PRO, DOA, EMA, and SGA algorithms, two TCSC devices were placed on branches (5, 4), (5, 27), (5, 4), and (2, 5), respectively.

TABLE IV
THE OPTIMAL VARIABLES OF CASE-1 AND CASE-2 OBTAINED FROM PRO ALGORITHM

Control variables	Max	Min	Case-1	Case-2
P_{THG2} (MW)	80	20	48.7234	79.9958
P_{THG5} (MW)	50	15	21.3335	50.0000
P_{THG8} (MW)	35	10	21.2588	35.0000
P_{THG11} (MW)	30	10	11.9726	29.9720
P_{THG13} (MW)	40	12	12.0000	39.1631
V_1(p.u)	1.1	0.95	1.0835	1.0632
V_2(p.u)	1.1	0.95	1.0642	1.0567
V_5(p.u)	1.1	0.95	1.0332	1.0385
V_8(p.u)	1.1	0.95	1.0378	1.0439
V_{11}(p.u)	1.1	0.95	1.0999	1.0984
V_{13}(p.u)	1.1	0.95	1.0689	1.0700
T_{11}(p.u)	1.1	0.9	1.0200	0.9800
T_{12}(p.u)	1.1	0.9	0.9000	1.0400
T_{15}(p.u)	1.1	0.9	0.9800	1.0000
T_{36}(p.u)	1.1	0.9	0.9600	0.9600
τ_{TCSC1}(%)	50%	0	27.3608	50.0000
τ_{TCSC1}(%)	50%	0	49.9999	23.8130
$TCSC_1$ branch, (con. buses):			**5, (2-5)**	**14, (9-10)**
$TCSC_2$ branch, (con. buses):			**4, (3-4)**	**5, (2-5)**
Total Cost ($/h)			**800.7291**	965.8169
Power loss (MW)			9.0971	**3.2629**
State variables				
P_{THG1} (MW)	200	50	177.2088	52.5321
Q_{THG1} (MVAr)	200	50	3.3587	-0.1942
Q_{THG2} (MVAr)	60	-20	20.5794	3.0035
Q_{THG5} (MVAr)	62.5	-15	25.9925	23.3088
Q_{THG8} (MVAr)	48.7	-15	36.5747	33.7850
Q_{THG11} (MVAr)	40	-10	26.5171	26.9927
Q_{THG13} (MVAr)	44.7	-15	14.5216	20.3510

The voltage values of the load buses are presented in Figure 3. Accordingly, these values were within the upper and lower bounds of the voltage limit. On the other hand, the lower and upper limit value ranges of control variables and reactive powers were given in Table 4. It is seen that the optimal solution values obtained from the PRO algorithm remained within this lower and upper limit ranges.

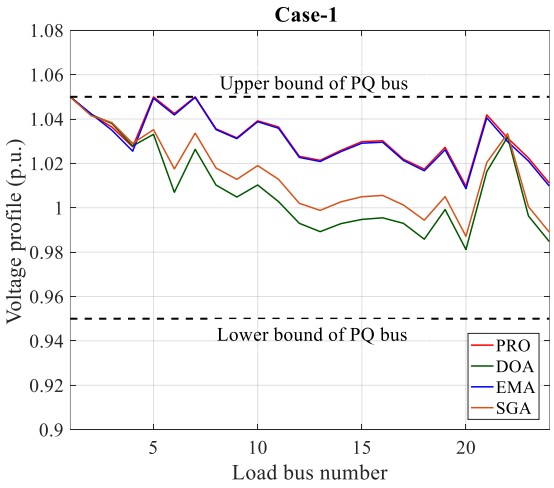

Figure 3. Voltage profiles of the load buses for all algorithms for Case-1

Case-2: *Minimization of the active power loss with TCSC*

The objective here was to place two TCSC devices in the most appropriate place while minimizing active power loss given in Eq. (20). The optimal variables obtained by the PRO algorithm for Case-2 are listed in Table 4. From Table 3, the

PRO algorithm yielded the minimum objective value of **3.2112 p.u.**, which was lower by **1.5863%**, **0.2814%**, and **1.1514%**, than the results of the DOA, EMA, and SGA algorithms, respectively. In this case, two TCSC devices were placed on the branches. Accordingly, TCSC devices were located on branches (14, 5), (25, 5), (7, 5), and (8, 5) according to the optimal results obtained from PRO, DOA, EMA and SGA algorithms, respectively. The voltage profiles of the load buses for all algorithms are shown in Figure 4, where these values remained within the specified voltage limits. Moreover, Table 4 provides the control variable and reactive power's lower and higher limit value ranges. According to these values, when the best solution values of the PRO algorithm were examined, it was seen that they remained within the valid limits.

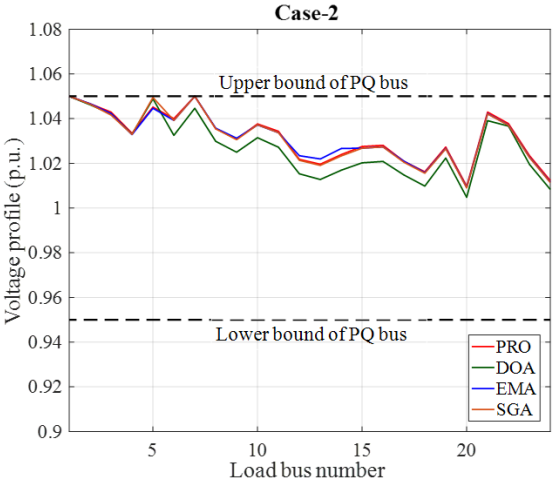

Figure 4. Voltage profiles of the load buses for all algorithms for Case-2

Case-3: *Minimization of the total cost with TCSC and TCPS*

The objective was to minimize the total cost given in Eq. (18), where two TCSC and two TCPS devices were included. The optimal variables identified by the PRO algorithm for Case-3 are tabulated in Table 5. It can be observed that all control variables were within the specified limits. When the results given in Table 3 were evaluated, the results obtained by PRO, DOA, EMA, and SGA were **800.6926 $/h**, **801.3040 $/h**, **800.7419 $/h**, and **801.0178 $/h,** respectively. These results clearly show that the result of PRO was **0.0763%**, **0.0062%**, and **0.0406%** lower than the DOA, EMA, and SGA algorithms, respectively. In this case, two TCSC and two TCPS devices were located on the branches. According to the optimal results obtained from PRO, DOA, EMA, and SGA algorithms, the TCSC devices were placed on branches (5, 13), (14, 13), (2, 1), and (39, 2), respectively. On the other hand, TCPS devices were located on branches (2, 6), (6, 8), (9, 1), and (5, 19) for the optimal results obtained from PRO, DOA, EMA, and SGA algorithms, respectively. The voltage profiles of the load buses for Case-3 are presented in Figure 5. It is demonstrated that the voltage values of the load buses remained within the specified upper and lower bounds. When examining whether the control variables given for Case-3 in Table 5 met the lower and upper limits, it was seen that all variables were within the specified limits.

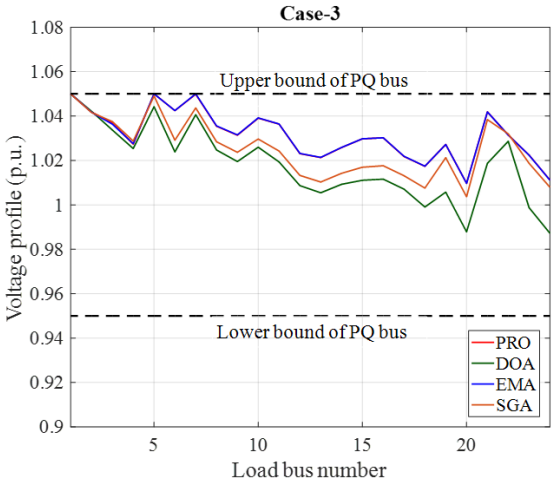

Figure 5. Voltage profiles of the load buses for all algorithms for Case-3

TABLE V
THE OPTIMAL VARIABLES OF CASE-3 AND CASE-4 OBTAINED FROM PRO ALGORITHM

Control variables	**Max.**	**Min.**	**Case-3**	**Case-4**
P_{THG2} (MW)	80	20	48.7512	42.6294
P_{THG5} (MW)	50	15	21.3364	19.3086
P_{THG8} (MW)	35	10	21.1918	10.1692
P_{THG11} (MW)	30	10	11.8607	10.0016
P_{THG13} (MW)	40	12	12.0001	12.0000
V_1 (p.u)	1.1	0.95	1.0827	1.0867
V_2 (p.u)	1.1	0.95	1.0635	1.0649
V_5 (p.u)	1.1	0.95	1.0323	1.0330
V_8 (p.u)	1.1	0.95	1.0363	1.0353
V_{11} (p.u)	1.1	0.95	1.0898	1.1000
V_{13} (p.u)	1.1	0.95	1.0686	1.0687
T_{11} (p.u)	1.1	0.9	1.0400	1.0200
T_{12} (p.u)	1.1	0.9	0.9000	0.9000
T_{15} (p.u)	1.1	0.9	0.9800	0.9800
T_{36} (p.u)	1.1	0.9	0.9600	0.9600
τ_{TCSC1}(%)	50%	0	27.2731	49.5061
τ_{TCSC1}(%)	50%	0	42.2571	29.3302
Φ_{TCPS1}	5	-5	-0.8802	-1.9422
Φ_{TCPS2}	5	-5	0.1184	-0.0201
$TCSC_1$ branch, (con. buses):			**5, (2-5)**	**4, (3-4)**
$TCSC_2$ branch, (con. buses):			**13, (9-11)**	**25, (10-20)**
$TCPS_1$ branch, (con. buses):			**2, (1-3)**	**8, (5-7)**
$TCPS_2$ branch, (con. buses):			**6, (26)**	**27, (10-21)**
Total Cost ($/h)			**800.6926**	**831.6959**
Power loss (MW)			9.0992	10.7089
State variables				
P_{THG1} (MW)	200	50	177.3591	199.9999
Q_{THG1} (MVAr)	200	50	2.9051	4.6583
Q_{THG2} (MVAr)	60	-20	19.6260	23.9679
Q_{THG5} (MVAr)	62.5	-15	25.1286	28.0478
Q_{THG8} (MVAr)	48.7	-15	30.8433	36.8284
Q_{THG11} (MVAr)	40	-10	36.2065	27.0314
Q_{THG13} (MVAr)	44.7	-15	14.3994	14.6355

Case-4: *Minimization of the total fuel cost with valve-point loading effect with TCSC and TCPS*

In this case, the objective was to minimize the total cost with VPLE given in Eq. (19), where two TCSC and two TCPS devices were located on the test system. The optimal variables obtained by the PRO algorithm for Case-4 are presented in Table 5. It is seen that all control variables were within the upper and lower bounds. The results of the PRO, DOA, EMA, and SGA algorithms presented in Table 3 were **831.6959 $/h**, **832.9082 $/h**, **831.6988 $/h**, and **831.9242 $/h**, respectively. Accordingly, the best objective function value was obtained from the PRO algorithm which was lower **0.1455%**, **0.0003%**, and **0.0274%** than the DOA, EMA, and SGA algorithms. In this case, according to the optimal results obtained from PRO, DOA, EMA, and SGA algorithms, the

TCSC devices were located on branches (4, 25), (22, 7), (5, 13), and (24, 29), and TCPS devices were located on branches (8, 27), (22, 34), (2, 1), and (8, 1), respectively. Figure 6 presents the voltage profiles of the load buses for all algorithms, illustrating that the load bus voltage levels stayed within the designated higher and lower boundaries. When the control variables obtained from the PRO algorithm for Case-4 given in Table 5 were evaluated in terms of whether they met the lower and upper limits, it was seen that they were within the limits.

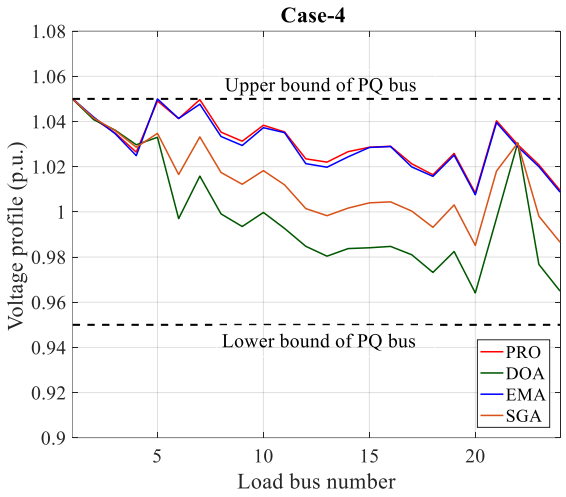

Figure 6. Voltage profiles of the load buses for all algorithms for Case-4

4.2. Convergence analysis

In order to evaluate the search performance of the PRO and its rival algorithms, the convergence graphs of them for all case studies were drawn. Since convergence graphs belong to the run in which the algorithms obtain the best solution, they do not fully reflect the search performance of the algorithms in solving the problem. Therefore, the box-plot graphs were drawn using the fitness values obtained by the algorithms as a result of 30 runs.

The convergence graphs and box-plots of all algorithms for Case-1 are shown in Figure 7. According to Figure 7 (a), the PRO algorithm demonstrated the best convergence performance compared to its competitors. Figure 7 (b) presents the box-plots for all algorithms. It is seen that the PRO algorithm had the smallest minimum, maximum, and median value, and therefore the mean value obtained as a result of 30 runs was the smallest among all algorithms. That is, the PRO algorithm obtained a stable search performance against its competitors.

The convergence graphs and box-plots of all algorithms for Case-2 are presented in Figure 8. From 8 (a), it is evident that the PRO algorithm converged to the lowest objective value among them. According to Figure 8 (b), it is clearly seen that the PRO algorithm had the smallest spread and therefore the smallest median and mean values among all algorithms. On the other hand, the DOA algorithm with the widest spread had the worst search performance.

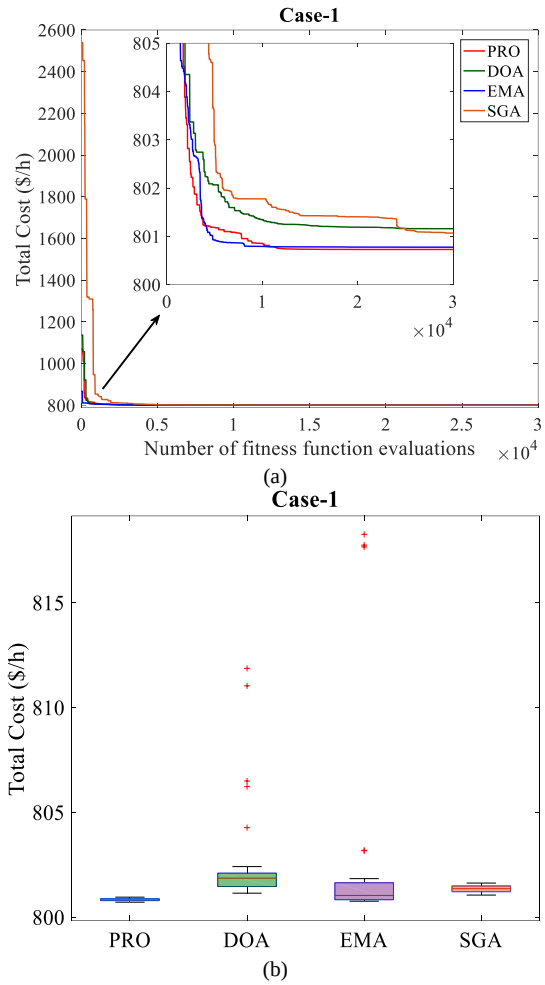

Figure 7. (a) Convergence graphs, (b) box-plots of all algorithms for Case-1

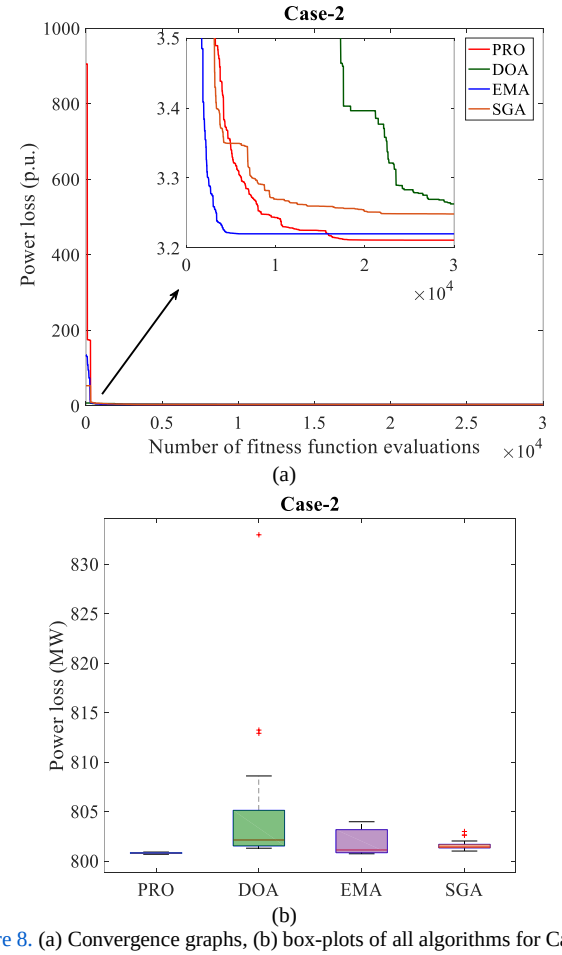

Figure 8. (a) Convergence graphs, (b) box-plots of all algorithms for Case-2

The convergence graphs of all algorithms for Case-3 are shown in Figure 9 (a). Accordingly, the PRO algorithm exhibited the best convergence performance in comparison to its competitors. The box-plots of all algorithms for Case-3 are shown in Figure 9 (b). While the PRO algorithm exhibited the best search performance, the DOA algorithm had the worst search performance among all algorithms.

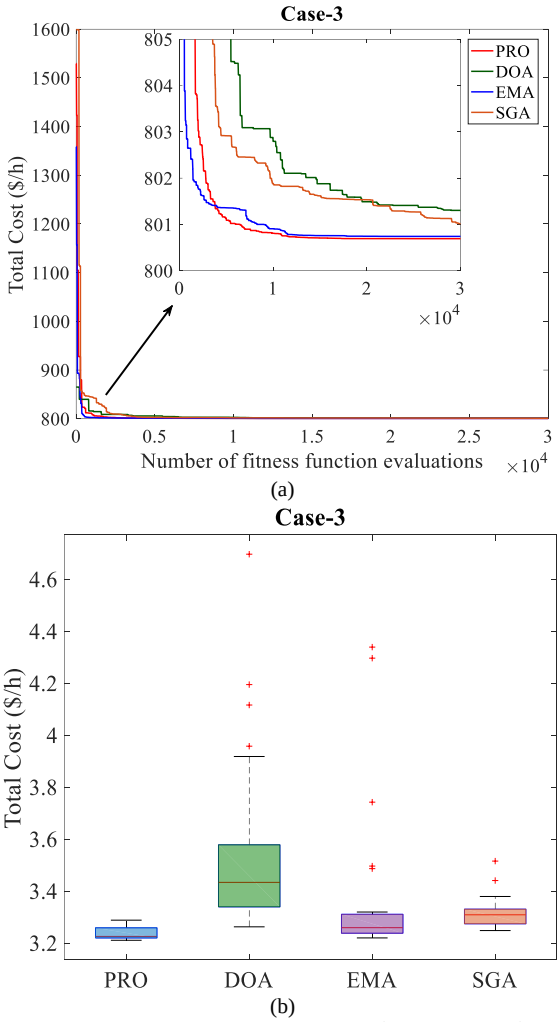

Figure 9. (a) Convergence graphs, (b) box-plots of all algorithms for Case-3

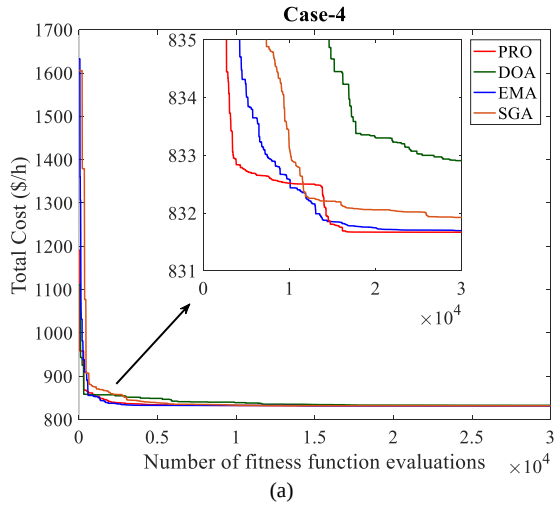

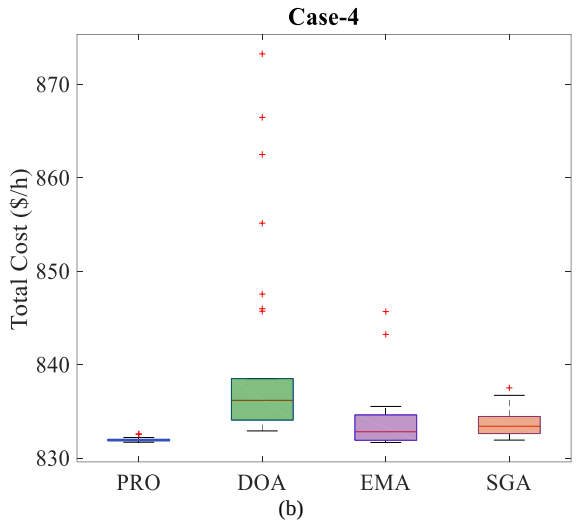

Figure 10. (a) Convergence graphs, (b) box-plots of all algorithms for Case-4

The convergence graphs of all algorithms for Case-4 are shown in Figure 10 (a). It can be seen that the PRO algorithm converged faster than its rivals. Figure 10 (b) presents the box-plots of all algorithms for Case-4. The PRO algorithm had the smallest minimum, maximum, median, and mean values for 30 independent runs. However, it is clear that DOA was the algorithm with the worst search performance due to its widest spread.

4.3. Statistical analysis

To analyze the performance of the algorithms, Friedman and Wilcoxon tests were applied on four case studies. The Friedman test provides broad information regarding the search performances of the algorithms, while the Wilcoxon test is used to determine the significance of the differences between the MHS algorithms, where the algorithms are compared pairwise. The Friedman score values of all algorithms are given in Figure 11. In the calculation of the score values given in Figure 11, the fitness function values obtained from the four case studies of the algorithms were used. From Figure 11, the score values of the PRO, DOA, EMA, and SGA algorithms were 1.2333, 3.6250, 2.3250, and 2.8167, respectively. That is, according to these results, the PRO algorithm ranked first, while the DOA algorithm ranked last.

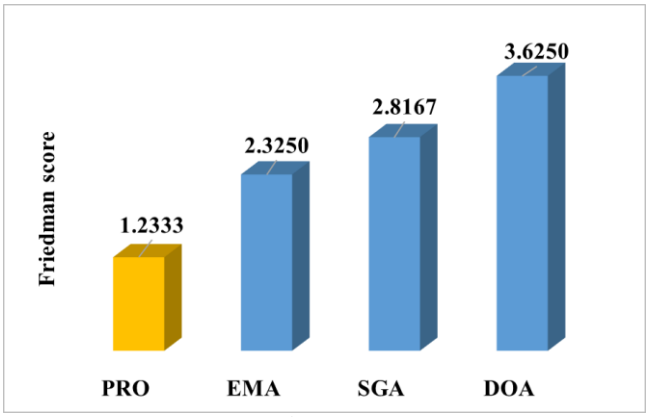

Figure 11. Friedman score values for all algorithms

Besides the Friedman test, the Wilcoxon test was performed to evaluate to performance of the algorithms in pairs. The Wilcoxon test was performed between the PRO algorithm and rival algorithms, and the results are presented

in Table 6. Here, the *Y*-value indicates the score based on the runs lost by the PRO algorithm, while the *Y*+ value represents the score based on the runs won by the PRO algorithm through pairwise comparisons of the results from 30 runs. Accordingly, the PRO algorithm outperformed its rivals in all case studies. To sum up, both Friedman and Wilcoxon test results proved the superior performance of the PRO algorithm over its competitors in four case studies.

TABLE VI
WILCOXON TEST RESULTS FOR ALL CASE STUDIES BETWEEN PRO AND OTHERS

Case(s)	*PRO vs. DOA*			*PRO vs. EMA*			*PRO vs. SGA*		
	Y-	*Y+*	*p-value*	*Y-*	*Y+*	*p-value*	*Y-*	*Y+*	*p-value*
Case-1	0	465	1.73e-06	25	440	1.97e-05	0	465	1.73e-06
Case-2	0	465	1.73e-06	32	433	3.72e-05	0	465	1.73e-06
Case-3	0	465	1.73e-06	51	414	1.89e-05	7	458	3.52e-06
Case-4	0	465	1.73e-06	61	404	1.29e-04	0	465	1.73e-06

5. CONCLUSION

This study presents the application of the partial reinforcement optimizer (PRO) algorithm for the solution of the OPF problem incorporating the optimal placement and sizing of the TCSC and TCPS devices. To solve the OPF problem, including the optimal placement of TCSC and TCPS devices, three objective functions were discussed. These were the minimization of total cost, the minimization of total cost with VPLED, and the minimization of active power loss. Using these objective functions and the TCSC and TCPS devices, four case studies were created. For the solution of these case studies, the performance of the PRO algorithm was compared with the up-to-date MHS algorithms, including DOA, EMA, and SGA. According to results of all algorithms, the PRO algorithm achieved a 0.0059%, 0.2814%, 0.0062 %, 0.0003% improvement over its closest competitor, the EMA algorithm, for Case-1, Case-2, Case-3, and Case-4, respectively. On the other hand, for the evaluation of the performance of all algorithms over the solution of these case studies, the statistical analysis methods were used. According to the results of the Friedman score, the PRO algorithm ranked first with 1.2333 score value against its competitors. Moreover, the Wilcoxon test results showed that the PRO algorithm outperformed its competitors in all case studies.

To sum up, the superiority of the PRO algorithm in solving the OPF problem incorporating the optimal placement and sizing of the TCSC and TCPS devices has been confirmed. In future studies, the PRO algorithm can be used to solve complex real-world problems.

REFERENCES

[1] S. Duman, "Solution of the optimal power flow problem considering FACTS devices by using lightning search algorithm", Iranian Journal of Science and Technology, Transactions of Electrical Engineering, vol. 43, pp. 969-997, Dec. 2019.

[2] M. H. Sulaiman and Z. Mustaffa, "Optimal placement and sizing of FACTS devices for optimal power flow using metaheuristic optimizers", Results in Control and Optimization, vol. 8, 100145, Sep. 2022.

[3] A. Mukherjee and V. Mukherjee, "Solution of optimal power flow with FACTS devices using a novel oppositional krill herd algorithm", International Journal of Electrical Power & Energy Systems, vol. 78, pp. 700-714, June 2016.

[4] E. Naderi, M. Pourakbari-Kasmaei, and H. Abdi, "An efficient particle swarm optimization algorithm to solve optimal power flow problem integrated with FACTS devices", Applied Soft Computing, vol. 80, pp. 243-262, July 2019.

[5] J. B. Edward, N. Rajasekar, K. Sathiyasekar, N. Senthilnathan, and R. Sarjila, "An enhanced bacterial foraging algorithm approach for optimal power flow problem including FACTS devices considering system loadability", ISA Transactions, vol. 52, no. 5, pp. 622-628, Sep. 2013.

[6] D. Prasad and V. Mukherjee, "A novel symbiotic organisms search algorithm for optimal power flow of power system with FACTS devices", Engineering Science and Technology, an International Journal, vol. 19, no. 1, pp. 79-89, March 2016.

[7] B. Mahdad, "Improvement optimal power flow solution considering SVC and TCSC controllers using new partitioned ant lion algorithm", Electrical Engineering, vol. 102, no. 4, pp. 2655-2672, Dec. 2020.

[8] M. Ebeed, A. Mostafa, M. M. Aly, F. Jurado, and S. Kamel, "Stochastic optimal power flow analysis of power systems with wind/PV/TCSC using a developed Runge Kutta optimizer", International Journal of Electrical Power & Energy Systems, vol. 152, 109250, Oct. 2023.

[9] M. A. Taher, S. Kamel, F. Jurado, and M. Ebeed, "Optimal power flow solution incorporating a simplified UPFC model using lightning attachment procedure optimization", International Transactions on Electrical Energy Systems, vol. 30, no. 1, e12170, Jan. 2020.

[10] P. P. Biswas, P. Arora, R. Mallipeddi, P. N. Suganthan, and B. K. Panigrahi, "Optimal placement and sizing of FACTS devices for optimal power flow in a wind power integrated electrical network", Neural Computing and Applications, vol. 33, pp. 6753-6774, June 2021.

[11] A. A. Ahmad and R. Sirjani, "Optimal placement and sizing of multi-type FACTS devices in power systems using metaheuristic optimisation techniques: An updated review", Ain Shams Engineering Journal, vol. 11, no. 3, pp. 611-628, Sep. 2020.

[12] S. R. Inkollu and V. R. Kota, "Optimal setting of FACTS devices for voltage stability improvement using PSO adaptive GSA hybrid algorithm", Engineering Science and Technology, An International Journal, vol. 19, no. 3, pp. 1166-1176, Sep. 2016.

[13] W. S. Sakr, R. A. El-Sehiemy, and A. M. Azmy, "Optimal allocation of TCSCs by adaptive DE algorithm", IET Generation, Transmission & Distribution, vol. 10, no. 15, pp. 3844-3854, Nov. 2016.

[14] S. R. Inkollu and V. R. Kota, "Optimal setting of FACTS devices for voltage stability improvement using PSO adaptive GSA hybrid algorithm", Engineering Science and Technology, An International Journal, vol. 19, no. 3, pp. 1166-1176, Sep. 2016.

[15] O. Ziaee and F. F. Choobineh, "Optimal location-allocation of TCSC devices on a transmission network", IEEE Transactions on Power Systems, vol. 32, no. 1, pp. 94-102, Jan. 2017.

[16] S. Raj and B. Bhattacharyya, "Optimal placement of TCSC and SVC for reactive power planning using Whale optimization algorithm", Swarm and Evolutionary Computation, vol. 40, pp. 131-143, June 2018.

[17] R. Agrawal, S. K. Bharadwaj, and D. P. Kothari, "Population based evolutionary optimization techniques for optimal allocation and sizing of Thyristor Controlled Series Capacitor", Journal of Electrical Systems and Information Technology, vol. 5, no. 3, pp. 484-501, Dec. 2018.

[18] N. H. Khan, Y. Wang, D. Tian, R. Jamal, S. Iqbal, M. A. A. Saif, and M. Ebeed, "A novel modified lightning attachment procedure optimization technique for optimal allocation of the FACTS devices in power systems", IEEE Access, vol. 9, pp. 47976-47997, Feb. 2021.

[19] K. Nusair, F. Alasali, A. Hayajneh, and W. Holderbaum, "Optimal placement of FACTS devices and power-flow solutions for a power network system integrated with stochastic renewable energy resources using new metaheuristic optimization techniques", International Journal of Energy Research, vol. 45, no. 13, pp. 18786-18809, Oct. 2021.

[20] A. A. Mohamed, S. Kamel, M. H. Hassan, M. I. Mosaad, and M. Aljohani, "Optimal power flow analysis based on hybrid gradient-based optimizer with moth–flame optimization algorithm considering optimal placement and sizing of FACTS/wind power", Mathematics, vol. 10, no. 3, pp. 361, Jan. 2022.

[21] M. H. Hassan, F. Daqaq, , S. Kamel, A. G. Hussien, and H. M. Zawbaa, "An enhanced hunter-prey optimization for optimal power flow with FACTS devices and wind power integration", IET Generation, Transmission & Distribution, vol. 17, no. 14, pp. 3115-3139, July 2023.

[22] A. Awad, S. Kamel, M. H. Hassan, and H. Zeinoddini-Meymand, "Optimal allocation of flexible AC transmission system (FACTS) for wind turbines integrated power system", Energy Science & Engineering, vol. 12, no. 1, pp. 181-200, Jan. 2024.

[23] A. A. Mohamed, S. Kamel, M. H. Hassan, and H. Zeinoddini-Meymand, "CAVOA: A chaotic optimization algorithm for optimal power flow with facts devices and stochastic wind power generation", IET Generation, Transmission & Distribution, vol. 18, no. 1, pp. 121-144, Jan. 2024.

[24] S. Mahapatra, N. Malik, S. Raj, and M. K. Srinivasan, "Constrained optimal power flow and optimal TCSC allocation using hybrid cuckoo search and ant lion optimizer", International Journal of System Assurance Engineering and Management, vol. 13, pp. 721-734, Apr. 2022.

[25] A. Taheri, K. RahimiZadeh, A. Beheshti, J. Baumbach, R. V. Rao, S. Mirjalili, and A. H. Gandomi, "Partial reinforcement optimizer: An evolutionary optimization algorithm", Expert Systems with Applications, vol. 238, 122070, March 2024.

[26] H. Peraza-Vázquez, A. F. Peña-Delgado, G. Echavarría-Castillo, A. B. Morales-Cepeda, J. Velasco-Álvarez, and F. Ruiz-Perez, "A bio-inspired method for engineering design optimization inspired by dingoes hunting strategies", Mathematical Problems in Engineering, vol. 2021, 9107547, 1-19, Sept. 2021.

[27] M. H. Sulaiman, Z. Mustaffa, M. M. Saari, H. Daniyal, and S. Mirjalili, "Evolutionary mating algorithm", Neural Computing and Applications, vol. 35, no. 1, pp. 487-516, Jan. 2023.

[28] A. Q. Tian, F. F. Liu, and H. X. Lv, "Snow Geese Algorithm: A novel migration-inspired meta-heuristic algorithm for constrained engineering optimization problems", Applied Mathematical Modelling, vol. 126, pp. 327-347, Feb. 2024.

[29] C. A. C. Coello, "Theoretical and numerical constraint-handling techniques used with evolutionary algorithms: a survey of the state of the art", Computer Methods in Applied Mechanics and Engineering, vol. 191, no. 11-12, pp. 1245-1287, Jan. 2002.

[30] C. B. Ferster and B. F. Skinner, Schedules of reinforcement. Appleton-Century-Crofts, 1957.

[31] The data of the IEEE 30-bus test system, http://labs.ece.uw.edu/pstca/pf30/pg_tca30bus.htm

[32] P. P. Biswas, P. N. Suganthan, R. Mallipeddi, and G. A. Amaratunga, "Optimal power flow solutions using differential evolution algorithm integrated with effective constraint handling techniques", Engineering Applications of Artificial Intelligence, vol. 68, pp. 81-100, Feb. 2018.

BIOGRAPHY

Burçin Özkaya obtained his BSc degree in Electrical and Electronics Engineering from Eskişehir Osmangazi University (ESOGU) in 2014. She received MSc. in Electrical and Electronics Engineering from the Süleyman Demirel University in 2018, and PhD degree in Electrical and Electronics Engineering from Düzce University in 2022. She worked as a Research Assistant with the Department of Electrical and Electronics Engineering at Suleyman Demirel University from 2015 to 2018, and with Department of Electrical and Electronics Engineering at Isparta University of Applied Sciences from 2018 to April 2023. She has been working as an Assistant Professor since April 2023 at Department of Electrical Engineering at Bandırma Onyedi Eylül University. Her research interests include power systems applications, optimization, meta-heuristic algorithms, and artificial intelligence.